Pergamon

Geochimica et Cosmochimica Acta, Vol. 62, No. 18, pp. 3087–3094, 1998

0016-7037/98 $19.00 + .00

PII S0016-7037(98)00215-4

Isotope-ratio-monitoring of O_2 for microanalysis of $^{18}O/^{16}O$ and $^{17}O/^{16}O$ in geological materials

EDWARD D. YOUNG,*[,1] MARILYN L. FOGEL,[2] DOUGLAS RUMBLE III,[2] and THOMAS C. HOERING[2]

[1]Department of Earth Sciences, University of Oxford, Oxford OX1 3PR, UK
[2]Geophysical Laboratory, 5251 Broad Branch Road, NW, Washington, D.C. 20015, USA

Abstract—Experiments were performed to test the viability of using isotope-ratio-monitoring gas-chromatography mass spectrometry (*irm*-GCMS) as a means for isotopic analysis of nanomole quantities of O_2 released in a vacuum system suitable for laser extraction and fluorination. Several sources of error were identified and eliminated, including false signals from extraneous scattered ions and adsorption of O_2 to metal surfaces. Results show that with appropriate attention to these potential impediments, coupling high-precision *irm*-GCMS to laser sampling of microgram quantities of silicate and oxide minerals is feasible. *Copyright © 1998 Elsevier Science Ltd*

1. INTRODUCTION

Considerable effort has been expended in recent years toward development of an oxygen isotope microprobe. Laser-based methods of O extraction combined with gas-source isotope ratio mass spectrometry (MS) offer the potential for spatial resolution commensurate with individual minerals in rocks and analytical precision sufficient for resolving differences in $^{18}O/^{16}O$ of several tenths of one part per thousand. The inability to measure the isotopic composition of small amounts of O released from mineral samples has been one of the most unremitting problems for those seeking to perform $^{18}O/^{16}O$ and $^{17}O/^{16}O$ microanalysis of silicates and oxides (e.g., Weichert and Hoefs, 1995; Rumble et al., 1997) and manipulation of small (e.g., nanomole) quantities of O_2 gas with isotope fidelity is often cited as the limiting factor in laser-based microanalysis of oxygen isotope ratios by fluorination (Valley et al., 1995).

We investigated the use of isotope-ratio-monitoring gas-chromatography mass spectrometry (*irm*-GCMS) as a means for measuring $^{18}O/^{16}O$ and $^{17}O/^{16}O$ of O_2 liberated by laser ablation and fluorination in nanomole quantities. The *irm*-GCMS method for O_2 analysis was investigated independent of laser extraction and fluorination procedures so that the causes of any fractionation incurred by the latter could be isolated from the effects of gas handling and mass spectrometry. Results show that O_2 samples corresponding to microgram quantities of silicate or oxide mineral material can be analyzed for both $^{18}O/^{16}O$ and $^{17}O/^{16}O$ with precision and accuracy similar to that of conventional dual-inlet MS methods. The *irm*-GCMS method has been used to develop a laser-based microprobe for oxygen isotopic analysis described elsewhere (Young et al., 1998).

2. THEORETICAL PRECISION

Determination of $^{18}O/^{16}O$ and $^{17}O/^{16}O$ by *irm*-GCMS amounts to measuring ratios of ion currents. Therefore, the maximum precision obtainable is limited by the reproducibility of ion current detection. Our repeated measurements of reference gases show that realizable uncertainties in oxygen isotope ratios determined by *irm*-GCMS are approximately double those imparted by current fluctuations known as shot noise (actual precision ranges from 1.4 to 2.3 times shot noise). These fluctuations are inherent in the statistics of counting discrete charges over a fixed time interval and are calculable. Instrument performance relative to shot noise can be used to predict real-world precision. With this in mind, estimates for the minimum silicate sample size that can be analyzed by *irm*-GCMS to a specified precision are obtained using the method of Hayes et al. (1977) and Merritt and Hayes (1994).

Convention dictates that uncertainties be expressed in terms of the δ notation (McKinney et al., 1950). For oxygen, the δ refers to the per mil (per thousandth) deviation in $^{18}O/^{16}O$ or $^{17}O/^{16}O$ of sample (x) relative to that of standard (std):

$$\delta^{17}O = ({}^{17}R^x/{}^{17}R^{std} - 1) \cdot 10^3 \quad (1)$$

$$\delta^{18}O = ({}^{18}R^x/{}^{18}R^{std} - 1) \cdot 10^3 \quad (2)$$

where $^{17}R^x$ and $^{17}R^{std}$ are $^{17}O/^{16}O$ for the unknown and the standard, respectively, and $^{18}R^x$ and $^{18}R^{std}$ are the analogous values for $^{18}O/^{16}O$. In practice ^{17}R and ^{18}R are represented by ratios of ion currents for m/z corresponding to the O_2 isotopomers $^{16}O^{16}O$, $^{18}O^{16}O$, $^{16}O^{18}O$, $^{17}O^{16}O$, $^{16}O^{17}O$, and $^{17}O^{17}O$. The three currents of interest are ^{32}I, ^{33}I, and ^{34}I. Ratios of ^{33}I and ^{34}I relative to ^{32}I are written as $^{33}R_i$ and $^{34}R_i$ and their relation to the isotope ratios of oxygen is straightforward if there are no interferences from other molecular or atomic species (Santrock et al., 1985):

$${}^{33}R_i = 2{}^{17}R \quad (3)$$

$${}^{34}R_i = 2{}^{18}R + {}^{17}R^2. \quad (4)$$

Expressions for uncertainties in measured δ values in terms of the total number of oxygen molecules admitted to the source are

$$\sigma^2_{\delta^{17}O} = \left(\frac{2 \times 10^6 (1 + {}^{33}R_i)(1 + {}^{33}R_i + {}^{34}R_i)}{{}^{33}R_i \, x_g \varepsilon M} \right)$$

$$\sigma^2_{\delta^{18}O} = \left(\frac{2 \times 10^6 (1 + {}^{34}R_i)(1 + {}^{33}R_i + {}^{34}R_i){}^{34}R_i}{\left({}^{34}R_i - \frac{{}^{33}R^2}{4} \right)^2 x_g \varepsilon M} \right) \quad (5)$$

*Author to whom correspondence should be addressed (ed.young@earth.ox.ac.uk).

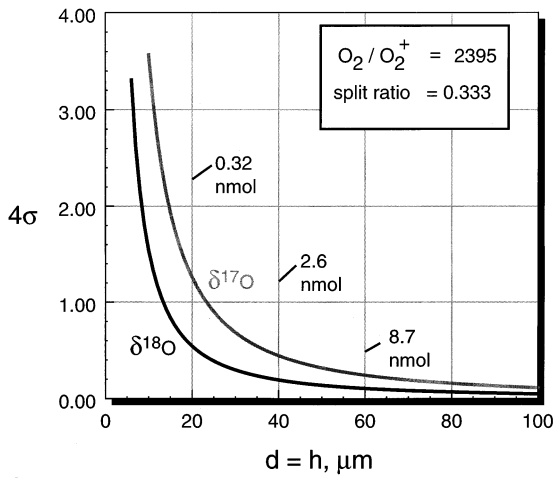

Fig. 1. Estimated precision for $\delta^{18}O$ and $\delta^{17}O$ as a function of silicate sample size. σ represents shot noise. 4σ corresponds to realizable 2σ. d is the diameter of a cylinder of silicate. h is the height of the cylinder.

where x_g is the fraction of sample gas that enters the source of the mass spectrometer, ε is the ionization efficiency of the source expressed as ions per molecule, and M is the total number of oxygen molecules comprising the sample.

Values of 0.00414 and 0.00075 for $^{33}R_i$ and $^{34}R_i$, respectively, are suitable for most geological materials (e.g., Nier, 1950), whereas ionization efficiency and sample fraction will vary from instrument to instrument. In the Oxford Earth Sciences stable isotope laboratory, the ionization efficiency for O_2 entrained in He has been measured and is 4.2×10^{-4}. The fraction of sample that enters the source via the open split is nominally 0.33. These values are taken to be representative of what can be obtained with modern instrumentation. Substitution of the measured values for ε and x_g and incorporation of Avogadro's number gives

$$\sigma^2_{\delta^{17}O} = \frac{0.03199}{n_{O_2}}$$

$$\sigma^2_{\delta^{18}O} = \frac{0.00581}{n_{O_2}} \quad (6)$$

where n_{O_2} is the amount of sample O_2 in nanomoles. Because actual precision is about two times shot noise, estimates of 2σ precision that can be expected when applying *irm*-GCMS to the extraction of O_2 from silicate minerals are obtained by multiplying the shot-noise $2\sigma_{\delta^{18}O}$ and $2\sigma_{\delta^{17}O}$ of Eqn. 6 by a factor of 2 (i.e., actual 2σ is equivalent to 4σ when σ refers to shot noise).

Figure 1 shows expected real-world precision (2σ) in $\delta^{18}O$ and $\delta^{17}O$ prescribed by Eqn. 6 as a function of the amount of silicate mineral analyzed. The quantity of mineral is expressed as the dimension of a cylinder of equal depth and diameter, a shape similar to many pits produced by laser ablation. From the curves in Fig. 1 it appears that the minimum volume of silicate that can be analyzed to a 2σ precision of $\pm 0.2‰$ in $\delta^{18}O$ would come from a pit measuring 39 μm in diameter, correspond to a sample weight of approximately 191 nanograms and yield 2.4 nanomoles of O_2 gas. The advantage of high precision afforded by *irm*-GCMS declines rapidly for smaller samples. Oxygen yield for these calculations is the median for most silicates of geological interest, and mineral stoichiometry has little affect on the results.

Calculations presented above suggest that *irm*-GCMS of O_2 should, in the absence of other analytical difficulties, enable high-precision oxygen isotopic analysis of silicate samples with a maximum three-dimensional spatial resolution of 40 μm. This conclusion is based solely on the amount of analyte gas, and so we note that enhancement in spatial resolution is feasible by excavating pits with varied aspect ratio. For example, the precision predicted for an equidimensional crater of 39 μm diameter would also apply to a pit with a diameter of 100 μm and a depth of only 6 μm. Background (blank) oxygen and other gas-handling factors potentially limit realizable minimum sample sizes as described below.

3. INSTRUMENTATION

The Oxford University on-line system (Fig. 2) comprises a laser-ablation fluorination vacuum extraction line evacuated with corrosive-grade turbomolecular and backing rotary pumps, a flow system for entraining O_2 into the He carrier gas, and an *irm*-GCMS instrument. The *irm*-GCMS instrument is composed of a Finnigan MAT 252 gas-ratio mass spectrometer, a Shimadzu GC-R1A gas chromatograph, and a GC-MS interface. The latter (GC II interface, Finnigan MAT) consists of an open split, reference gas inlet, and Nafion water-removal assembly. The open split is described by Merritt et al. (1994). Tank reference gas injections are obtained by operation of an automated mixing volume also described by Merritt et al. (1994).

The cryofocusing device, also described as a preconcentration device, for transferring O_2 from the evacuated sample loop to flowing He is shown in Fig. 3. With the exception of the sample loop, for which a He purged valve is used, carrier gas flow is controlled by fixed lengths of fused silica capillary tubing acting as flow restrictors and two pneumatically-controlled on-off valves. Alternation of on-off valves 1 and 2 (Fig. 3) effects reversal of He flow through the cryofocus trap. Benefits of flow reversal were described by Klemp *et al.* (1993). The cryofocus trap consists of a 150 mm length of 1/32″ od stainless steel tube filled with silica gel that was sieved to -250 μm $+$ 150 μm and secured with Ni wool.

A porous layer open tubular (PLOT) fused silica GC separation column is used in the sample path upstream of the water removal membrane in order to purify O_2. The column has a 0.53 mm internal diameter, is 10 m in length, and is coated with 5A molecular sieve adsorbent (manufactured by Chrompak). Operating temperature was constant at 50°C for all experiments reported here. He flow rate through the column is 2 mL/min.

4. TEST OXYGEN GASES

All $\delta^{18}O$ and $\delta^{17}O$ values are reported relative to standard mean ocean water (SMOW). Oxygen from air was adopted as a primary standard for this study with a nominal value for $\delta^{18}O$ of $23.5 \pm 0.3‰$ (Craig, 1972). Two tanks of pure O_2 gas (grade 5.0) were used as secondary standards. All standard tank gas $\delta^{18}O$ values were determined by conventional dual-inlet viscous leak MS methods. Tank 1 $^{18}O/^{16}O$ was calibrated by quantitative reaction with hot graphite to form CO_2 followed by comparison with the Geophysical Laboratory CO_2 reference gas. The $^{18}O/^{16}O$ of Tank 2 was obtained by measurements relative to Tank 1 and confirmed by measurement against O_2 from air. Tank 2 was used as the Oxford reference gas.

Calibration of $^{17}O/^{16}O$ was performed by iterative comparison between models for mass-dependent fractionation and measured $^{18}O/^{16}O$ and $^{17}O/^{16}O$ of geological samples. This method is regarded as the most prudent means for assigning $\delta^{17}O$ for standard gases (R. N. Clayton, pers. commun. 1998). Mass-dependent fractionation leads to an array in a plot of $\delta^{18}O$ (abscissa) against $\delta^{17}O$ (ordinate). A mass fractionation

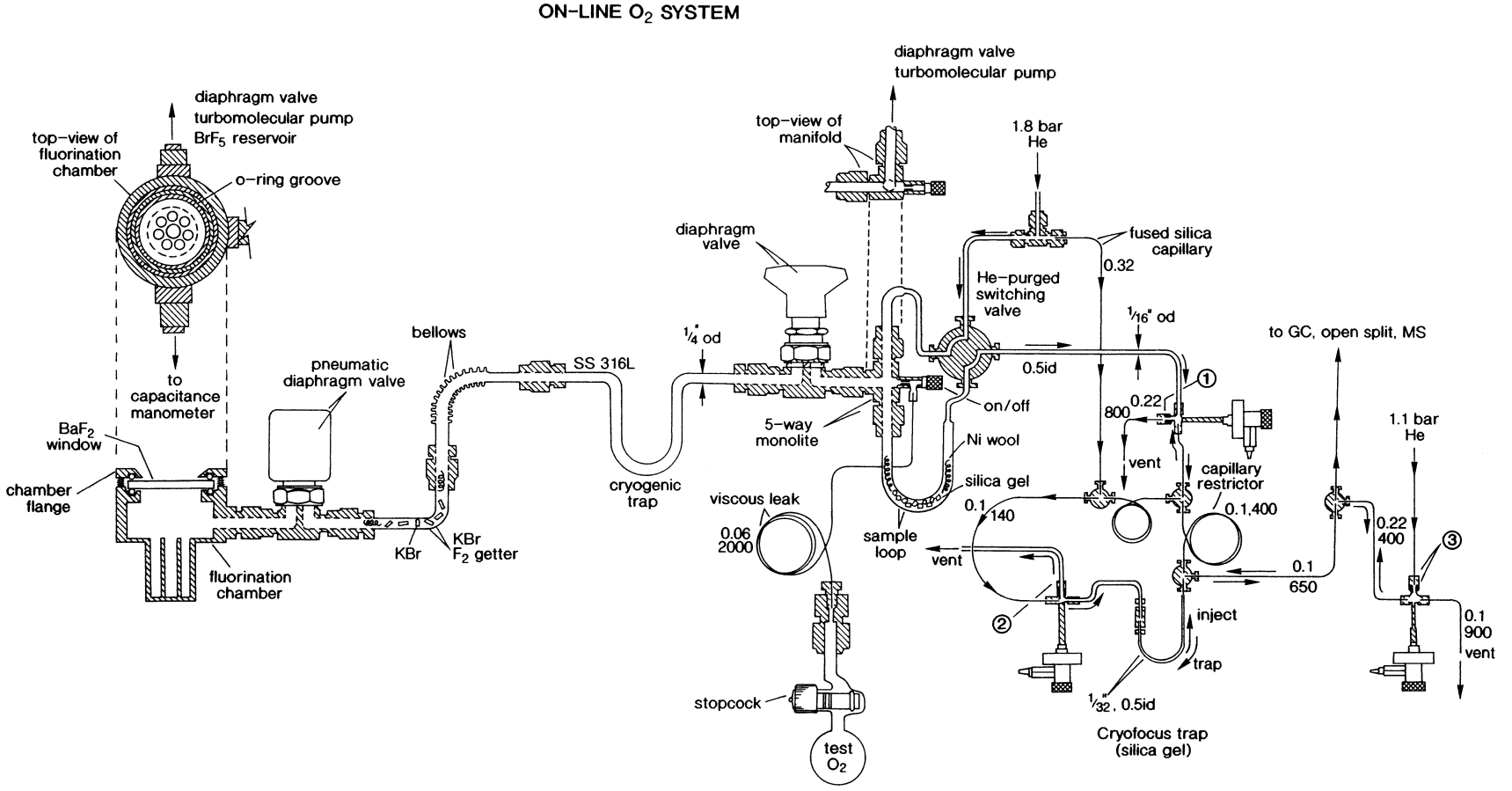

Fig. 2. Partial cutaway diagram of vacuum fluorination line. He plumbing is composed of stainless steel tubing (double lines) or fused silica capillary (single lines). Internal diameter and lengths are given in mm. Units for other dimensions are as specified.

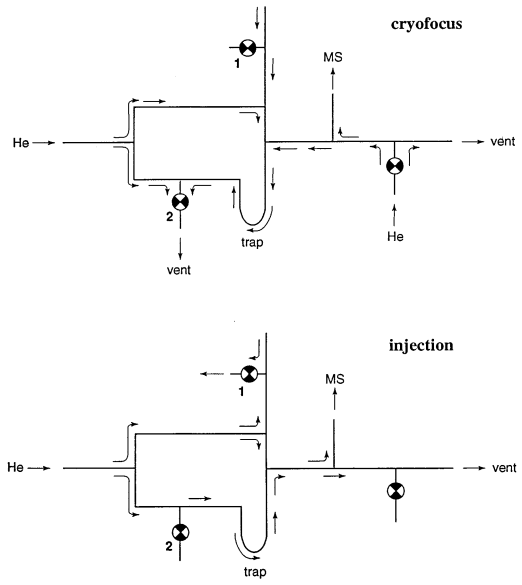

Fig. 3. Schematic diagram of He flow system for O_2 sample trapping and injection into the *irm*-GCMS system. Lines represent fused silica or stainless steel capillary tubing. Circles represent valves. Open valves are shown with white quadrants adjacent tubing. Closed valves are shown with black quadrants adjacent tubing. MS marks the fused silica tube connecting to the mass spectrometer.

array relating terrestrial materials can be described by the equation (Santrock et al., 1985)

$$^{17}R = {}^{18}R^{a} \cdot k \tag{7}$$

where $k = 0.04103a - 0.011387$. Kinetic theory (e.g., Bigeleisen, 1965) predicts that the parameter a will depend upon the physicochemical process involved. Values for a are expected to range from 0.500, representing the asymptotic limit where the effective molecular weights of the fractionating species containing oxygen are very large, to 0.529 for atomic oxygen. The terrestrial $\delta^{18}O$–$\delta^{17}O$ array is therefore a family of concave downward curves emanating from the origin and with each curve defined by a single value for a. As a result, predictions on the basis of mass fractionation could not be used to define $^{17}O/^{16}O$ for test gases directly from their $^{18}O/^{16}O$ values. Instead, the $^{17}O/^{16}O$ for Tank 2, the reference gas, was determined by requiring that measured $\delta^{18}O$ and $\delta^{17}O$ for oxygen obtained by laser ablation and fluorination of silicate minerals (Young et al., 1998) and biogenic phosphates (unpubl. data of Jones et al., 1998) define an average terrestrial mass fractionation curve with $a = 0.516$ (the average value for a is derived by Matshuhisa et al., 1978). The isotopic compositions of geological samples and Tank 1 lie on the curve, within error, when $\delta^{17}O$ for Tank 2 is -0.4 per mil below the curve. Deviations of tank O_2 $^{18}O/^{16}O$ and $^{17}O/^{16}O$ from the average terrestrial curve have been observed previously (R. N. Clayton, pers. commun. 1998). In order to relate Tank 2 $^{17}O/^{16}O$ to its $^{18}O/^{16}O$ with Eqn. 7, the value for a would have to be 0.470. This is lower than the 0.500 limit imposed by simple kinetic theory, suggesting that mixing between a highly fractionated oxygen (a byproduct of the manufacturing process) and oxygen with $^{18}O/^{16}O$ and $^{17}O/^{16}O$ closer to terrestrial geological values is the likely explanation for the offset between Tank 2 and the average terrestrial curve. For example, 1.45% residuum with $\delta^{18}O$ of 500.0 per mil and $\delta^{17}O$ of 232.7 per mil, lying on the average terrestrial curve, mixed with SMOW oxygen ($\delta^{18}O = \delta^{17}O = 0$), also on the average curve, gives the isotopic composition of Tank 2.

Aliquotes of Tank 1 and Tank 2 O_2 were admitted from a glass reservoir to the high vacuum system of the on-line apparatus using a 2-m length of 0.06 mm od fused silica capillary tubing (Fig. 2). A high-vacuum shutoff valve (SMOV, manufactured by SGE) connects the capillary tube to the sample loop of the vacuum system. Pressure in the glass reservoir was maintained above 140 mbar.

Nominal sample sizes were determined from peak areas by application of the equation

$$^{32}A = n_{O_2}\,(6.023 \times 10^{14} e\, x_g\, \varepsilon R) \tag{8}$$

where ^{32}A is the area (V · sec) for the m/z 32 peak, R is the magnitude of the major-beam collector amplifier feedback resistor (Ω), n_{O_2} is the amount of sample gas in nanomoles, and the other terms are defined above. Accuracy of calibrations based on Eqn. 8 is limited by uncertainties in x_g arising from adjustments in He flow rates. Application of Eqn. 8 for the experiments reported here yields $n_{O_2} = 0.62(^{32}A)$. We note that for *irm*-GCMS, just as for other MS applications, ionization efficiency of O_2 is about 0.6 that of CO_2.

5. RESULTS AND DISCUSSION

Results presented below demonstrate that nanomole quantities of O_2 gas can be collected in a vacuum extraction system and analyzed to yield accurate and precise $^{18}O/^{16}O$ and $^{17}O/^{16}O$ by *irm*-GCMS.

5.1. Test gases

Influences of different segments of the extraction line were isolated by measuring $\delta^{18}O$ and $\delta^{17}O$ after: (1) expansion to the sample loop with no trapping in the sample loop; (2) expansion followed by freezing to silica gel in the sample loop; (3) expansion through the cold trap and fluorine getter of the vacuum extraction line followed by collection on the sample-loop silica gel; (4) expansion through the extraction line to the fluorination chamber followed by collection onto the sample-loop silica gel; and (5) expansion to the fluorination chamber and mixing with BrF_5 (fluorinating reagent) prior to collection onto the sample-loop silica gel. The latter procedure was used to test the efficiency with which fluoride products are separated from analyte oxygen by the GC system and to test the effectiveness of the high-conductance KBr F_2 getter in protecting the downstream silica gel traps. Bromine pentafluoride, which disassociates to yield small amounts of F_2 upon reaction in vacuum lines, was used as the fluorinating agent for these experiments because, unlike F_2, it could be frozen in to the sample chamber at low pressures.

All samples were concentrated by cryofocusing at a flow rate of 3 mL/min. The design of the cryofocus trap permitted determination of the minimum trapping time by monitoring $m/z = 32$ just after flow reversal. Gas not yet trapped lingers in the capillary restrictors (Fig. 3) and appears as a broad rise in background prior to elution of the cryofocused peak. From this method it was determined that 10 min. is the minimum time required for complete trapping. Freezing times from the vacuum extraction line to the sample loop trap are discussed below.

A typical O_2 *irm*-GCMS output is shown in Fig. 4. The first square-topped peak is the reference gas injected directly into the source of the mass spectrometer by way of the mixing volume. Virtually no shift in the voltage ratios (representing $^{33}I/^{32}I$ and $^{34}I/^{32}I$) is observed for this peak because a bias was applied so that background ratios approximate those of the reference gas. The next peak to appear is another aliquot of the reference O_2 gas. In this case the gas was admitted to the sample loop by flow through the standard-gas capillary, cryofocused onto silica gel, passed through the GC column, and

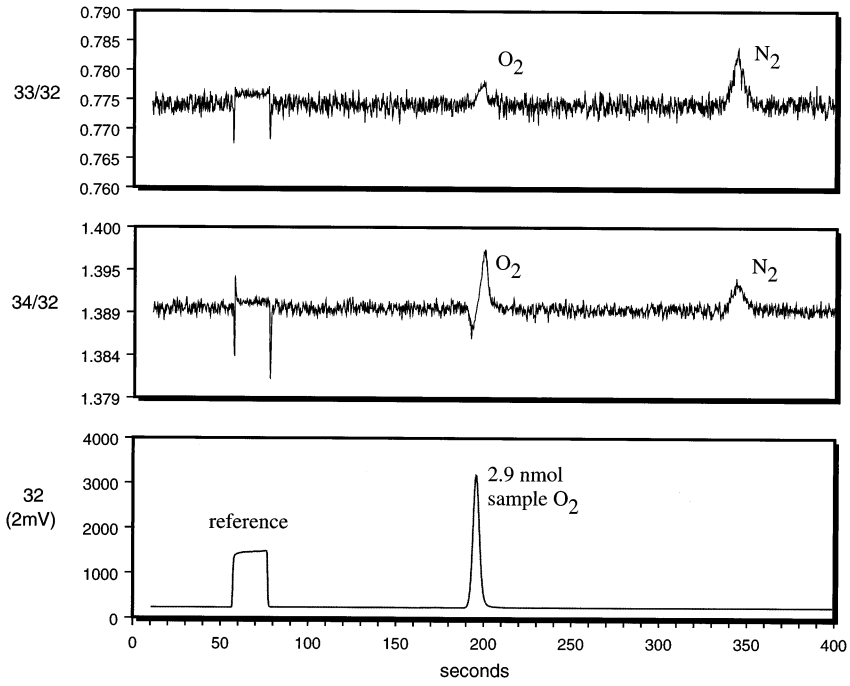

Fig. 4. Mass-specific chromatograms for *irm*-GCMS on-line run number 737. The $\delta^{18}O$ value for the Tank 2 reference gas is 7.3‰ (first peak). The $\delta^{18}O$ value for the 2.9 nmol sample of Tank 2 O_2 injected by cryofocusing is 8.2‰ (second peak). Correction for blank gives a $\delta^{18}O$ value of 7.4‰ for the cryofocused peak (Table 2).

finally injected into the mass spectrometer source. Voltage ratios vary from low to high relative to the reference gas ratio as the pulse of oxygen passes. The change from low to high ratios reflects greater adsorption of $^{33}O_2$ and $^{34}O_2$ relative to $^{32}O_2$ onto the 5A molecular sieve column. This normal isotope effect, in which the lighter species elute first, arises from dominance of motions of whole O_2 molecules in the adsorbed state over surface-adsorbate interactions and/or substantial stiffening of adsorbed O_2 intramolecular vibrations caused by the polar molecular sieve (Van Hook, 1967). It contrasts with the reverse isotope effect that obtains for CO_2 passed through various separation columns in other *irm*-GCMS applications. Efficacy of open tubular columns for separation of different isotopic molecules of O_2 has been documented previously (Bruner et al., 1966). Integration of the continuously varying voltage ratios yields $^{18}O/^{16}O$ and $^{17}O/^{16}O$ identical (within 0.1‰) to the baseline reference gas ratio after correction for blank.

The final peak in Fig. 4 arrives approximately 150 sec after the cryofocused oxygen. Monitoring of m/z during injections shows this to be a false oxygen signal caused by N_2. Virtually no false signal is evident for $m/z = 32$ while the 33 signal is always three times larger than the 34 signal. Feedback resistances for the 32, 33, and 34 collector amplifiers are $3 \times 10^8\Omega$, $3 \times 10^{11}\Omega$, and $1 \times 10^{11}\Omega$, respectively. As the sizes of the false peaks are proportional to the sensitivity of the collectors, we interpret the spurious peaks as being the result of scattering of N_2 ions toward the collectors. False $^{18}O/^{16}O$ and $^{17}O/^{16}O$ typically yield $\delta^{17}O$ values of 211‰ and $\delta^{18}O$ values of 72‰. As a result, coelution of N_2 and O_2 can cause significant errors in oxygen isotope ratio determinations for small samples. Omission of the column results in large and systematic apparent deviations in $\delta^{17}O$ and scatter in both $\delta^{17}O$ and $\delta^{18}O$. Separation of N_2 from O_2 using the 5A mol sieve column eliminates excursions in $\delta^{17}O$ and greatly reduces the scatter in the data. Purification of analyte O_2 by GC after cryofocusing is necessary for accurate measurements of isotope ratios for sample sizes on the order of several nanomoles.

Analyses of Tanks 1 and 2 obtained with the *irm*-GCMS system are summarized in Table 1 and Table 2. These data were collected after steps were taken to minimize sources of error discussed below and are indicative of the accuracy and precision of the present technique. Tank 1 proved useful because its $^{18}O/^{16}O$ is far removed from that of the blank and so the influence of the latter was magnified. The $^{18}O/^{16}O$ of Tank 2 is more representative of most terrestrial silicate and oxide samples. Results for all tank O_2 samples, ranging in size from 2 to 15 nanomoles, are accurate to within 0.1‰ (1σ) after correction for blank. Precision is also acceptable, yielding ± 0.4‰ for Tank 1 $\delta^{18}O$ (1σ, $n = 23$) and ± 0.07‰ for Tank 2 $\delta^{18}O$ (1σ, $n = 6$). On the basis of clusters of data exhibiting superior reproducibility, we suspect that the precision for Tank 1 could be improved with refinements in methods (e.g., improved methods for controlling blank).

System blank was generally on the order of 1 nanomole but ranged from a low of 0.7 nmol to a high of 1.9 nmol. Blank peaks are completely obscured by sample peaks, making curve fitting for blank subtraction of dubious benefit. This poses no difficulty, however, because the blank is sufficiently constant in both size and isotopic composition that corrections can be made by simple mass balance (Fig. 5). Blank from cryofocusing alone is on the order of 1 nanomole, indicating that the vast

Table 1. Results of experiments for Tank 1. All values for $\delta^{18}O$ and $\delta^{17}O$ are relative to SMOW. Accepted values are 48.0‰ and 24.5‰, respectively.

Run	Meas[1] $\delta^{18}O$	Meas[1] $\delta^{17}O$	Total nmol	Blank $\delta^{18}O$	Blank $\delta^{17}O$	Blank nmol	Corr.[2] $\delta^{18}O$	Corr.[2] $\delta^{17}O$	Method code[3]
763	43.46	22.51	8.67	11.79	5.26	1.03	47.73	24.83	SL
764	43.98	22.51	9.46	11.79	5.26	1.03	47.89	24.62	SL
765	44.08	22.49	9.40	11.79	5.26	1.03	48.04	24.61	SL
766	43.92	22.53	9.75	11.79	5.26	1.03	47.70	24.57	SL
767	43.54	21.89	9.88	11.79	5.26	1.03	47.22	23.82	SL
770	46.50	23.91	15.40	8.99	5.32	0.72	48.35	24.83	SLSG
771	46.61	24.32	15.29	8.99	5.32	0.72	48.48	25.26	SLSG
776	43.97	22.25	8.82	10.51	6.43	0.98	48.15	24.23	SL
777	43.56	22.15	9.40	10.51	6.43	0.98	47.40	23.98	SL
788	42.98	21.93	8.52	11.69	5.69	1.05	47.39	24.22	SL
791	45.57	23.34	13.52	11.69	5.69	1.05	48.43	24.82	SLSG
792	45.12	23.00	13.27	11.69	5.69	1.05	48.00	24.49	SLSG
810	44.76	22.53	11.56	11.29	4.39	1.01	47.97	24.27	SLSG
813	44.70	22.19	11.67	11.58	5.49	1.03	47.92	24.82	VL
814	45.24	22.86	11.19	10.86	5.24	0.91	48.28	25.42	VL
816	44.58	22.91	11.62	10.86	5.24	0.91	47.44	24.41	VL
817	45.15	22.7	11.28	11.13	5.44	0.90	48.08	24.19	VL
823	42.50	21.64	11.71	11.53	5.78	1.81	48.15	24.54	VLC
824	42.42	21.28	12.00	11.53	5.78	1.81	47.90	24.03	VLC
828	45.23	22.87	11.00	9.84	4.19	0.84	48.13	24.40	SLSG
830	42.56	21.94	11.81	10.54	5.51	1.60	47.57	24.51	VLC
831	42.25	21.70	11.77	10.54	5.51	1.60	47.24	24.25	VLC
841	41.43	21.38	10.51	11.43	4.74	1.89	48.03	25.04	VLC + BrF_5
avg[4]							47.89 ±0.37	24.44 ±0.37	

[1] Measured values inclusive of blank.
[2] Tank 2 analyses corrected for blank using peak areas in V · sec (areas not shown).
[3] SL = collection from sample loop only; SLSG = collection from sample loop silica gel; VL = collection from vacuum line; VLC = collection from vacuum line and fluorination chamber; VLC + BrF_5 = collection from vacuum line and fluorination chamber after mixing with BrF_5.
[4] Mean and 1σ for all Tank 1 analyses.

majority of extraneous oxygen comes from the He flow system rather than from the evacuated extraction line.

There is a 0.3‰ downward shift in mean $\delta^{18}O$ for Tank 1 obtained by expansion to the sample loop *without* freezing to silica gel relative to the mean obtained by cryogenic trapping. The negative shift was accompanied by a deficit of approximately 30% in O_2 peak areas relative to trapping experiments (compare the first eight results in Table 1). Apparently, purging the sample loop for 10 min (the normal time required for cryofocusing) is insufficient to flush all of the analyte gas from the sample loop assembly unless it is first concentrated on to silica gel.

Adsorption of O_2 on to the surfaces of the stainless steel cryogenic trap (Delchar et al., 1967) located between the fluorination chamber and the sample loop caused a buildup of oxygen on the trap walls after passage of several samples. As a result, when the trap was kept cold, blank size was observed to increase progressively throughout the day until it had more than doubled. Under these conditions the blank could no longer be considered constant and the precision of blank-corrected

Table 2. Results of experiments for Tank 2. All values for $\delta^{18}O$ and $\delta^{17}O$ are relative to SMOW. Accepted values are 7.3‰ and 3.4‰, respectively.

Run	Meas[1] $\delta^{18}O$	Meas[1] $\delta^{17}O$	Total nmol	Blank $\delta^{18}O$	Blank $\delta^{17}O$	Blank nmol	Corr.[2] $\delta^{18}O$	Corr.[2] $\delta^{17}O$	Method code[3]
750	7.71	3.66	8.54	10.67	6.01	0.92	7.35	3.38	SL
738	8.28	3.86	2.54	10.0[5]	4.75[5]	0.83[5]	7.45	3.43	SL
737	8.17	4.08	2.87	10.0[5]	4.75[5]	0.83[5]	7.43	3.81	SL
731	8.06	3.30	2.91	10.0[5]	4.75[5]	0.83[5]	7.29	2.73	SL
746	7.64	3.43	6.40	10.0[5]	4.75[5]	0.83[5]	7.29	3.23	SL
000	7.74	3.41	5.19	10.0[5]	4.75[5]	0.83[5]	7.31	3.16	SL
avg[4]							7.35 ±0.07	3.29 ±0.36	

[1] Measured values inclusive of blank.
[2] Tank 4 analyses corrected for blank using peak areas in V · sec (areas not shown).
[3] SL = collection from sample loop.
[4] Mean and 1σ for all Tank 2 analyses.
[5] Average blank over period of analyses.

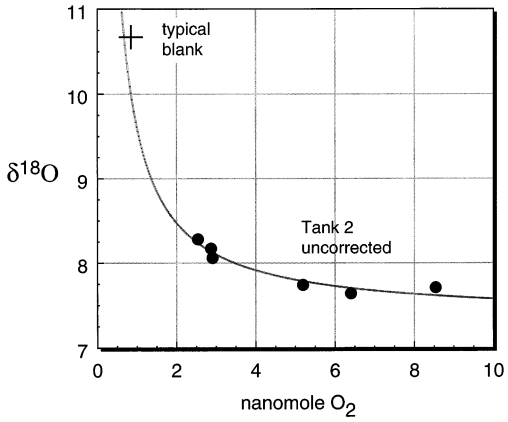

Fig. 5. Plot of measured $\delta^{18}O$ and sample size for on-line *irm*-GCMS analyses of Tank 2 prior to blank correction (solid circles). Grey line is the hyperbolic best fit to the data. Mixing between a single blank and Tank 2 would yield a perfect hyperbolic curve. The correlation coefficient of 0.969 for this fit is indication that the blank for these runs was effectively constant in both size and $\delta^{18}O$ value. Cross shows typical measured blank values.

results declined. The problem was solved by heating the trap to 423 K between samples.

5.2. Effects of fluorination

Results of experiments on O_2 test gases have been used to develop an oxygen isotope microprobe based on UV laser ablation and fluorination. The details of the UV laser ablation-fluorination system connected to the on-line system at Oxford University are presented elsewhere (Young et al., 1998). We mention here, however, that fluorination experiments revealed that the use of a separation column simplifies measurement of $\delta^{17}O$.

Gaseous fluorides can adversely affect the accuracy and precision of $\delta^{17}O$ measurements (Clayton and Mayeda, 1983). These fluorides are present as products of fluorination by either BrF_5 or F_2. Analysis by conventional MS requires a purification procedure involving cryogenic separation of O_2 from potential fluoride contaminants, especially NF_3. In combination with laser ablation-fluorination (using purified F_2), the *irm*-GCMS method described here yields $\delta^{17}O$ and $\delta^{18}O$ values of terrestrial samples relative to SMOW that are consistent with the average terrestrial mass fractionation line within 1σ uncertainties without additional purification of the analyte gas. Similarly, analyses of meteoritical samples lying off the terrestrial line are analyzed with accuracy in both $\delta^{18}O$ and $\delta^{17}O$ (Young et al., 1998).

6. CONCLUSIONS

The experiments described here show that *irm*-GCMS can be used to analyze nanomole quantities of O_2 gas for $^{18}O/^{16}O$ and $^{17}O/^{16}O$ with accuracy and precision suitable for geochemical applications, including high-temperature studies in which variations in $\delta^{18}O$ of $<1‰$ are important and investigations of meteoritical materials where relations between $\delta^{18}O$ and $\delta^{17}O$ are crucial. Critical aspects of the analytical method are gas purification by gas chromatography to preclude false signals from interfering ions and periodic cleaning of cryogenic traps to remove adsorbed oxygen. When combined with laser ablation and fluorination, *irm*-GCMS can be used to obtain *in situ* high-precision oxygen isotope ratio analyses of microgram quantities of silicate minerals.

Acknowledgments—The first author wishes to thank the Carnegie Institution of Washington's Geophysical Laboratory for support as a postdoctoral fellow during the early stages of this study. Professor R. N. Clayton kindly shared with us his experiences regarding calibration of $^{17}O/^{16}O$. Thoughtful reviews by Professor J. W. Valley and Dr. Z. D. Sharp are greatly appreciated.

REFERENCES

Bigeleisen J. (1965) Chemistry of isotopes. *Science* **147,** 463–471.

Bruner F., Cartoni G. P., and Liberti A. (1966) Gas chromatography of isotopic molecules on open tubular columns. *Anal. Chem.* **38,** 298–303.

Clayton R. N. and Mayeda T. K. (1983) Oxygen isotopes in eucrites, shergottites, nakhlites, and chassignites. *Earth Planet. Sci. Lett.* **62,** 1–6.

Craig H. (1972) Atmospheric oxygen: Isotopic composition and solubility fractionation. *Science* **175,** 54–55.

Delchar T. A. and Tompkins F. C. (1967) Chemisorption and incorporation of oxygen at a nickel surface. *Proc. Royal Soc.* **300,** 141–158.

Hayes J. M., DesMarais D. J., Peterson D. W., Schoeller D. A., and Taylor S. P. (1977) High precision stable isotope ratios from microgram samples. *Adv. Mass Spectrom.* **7A,** 475–480.

Jones A. M., Iacumin P., and Young E. D. (1998) High-resolution $\delta^{18}O$ analysis of biogenic phosphate by GC-*irms* and UV laser fluorination. *Chem. Geol.* (submitted).

Klemp M. A., Akard M. L., and Sacks R. D. (1993) Crofocusing inlet with reverse flow sample collection for gas chromatography. *Anal. Chem.* **65,** 2516–2521.

Matsuhisa Y., Goldsmith J. R., and Clayton R. N. (1978) Mechanisms of hydrothermal crystallization of quartz at 250°C and 15 kbar. *Geochim. Cosmochim. Acta* **42,** 173–182.

McKinney C. R., McCrea J. M., Epstein S., Allen H. A., and Urey H. C. (1950) Improvements in mass spectrometers for the measurement of small differences in isotope abundance ratios. *Rev. Sci. Instr.* **21,** 724.

Merritt D. A. and Hayes J. M. (1994) Factors controlling precision and accuracy in isotope-ratio-monitoring mass spectrometry. *Anal. Chem.* **66,** 2336–2347.

Merritt D. A., Brand W. A., and Hayes J. M. (1994) Isotope-ratio monitoring gas chromatography-mass spectrometry: methods for isotopic calibration. *Org. Geochem.* **21,** 573–583.

Nier A. O. (1950) A redetermination of the relative abundances of the isotopes of carbon, nitrogen, oxygen, argon, and potassium. *Phys. Rev.* **77,** 789–793.

Rumble D. III, Farquhar J., Young E. D., and Christensen C. P. (1997) In situ oxygen isotope analysis with an excimer laser using F_2 and BrF_5 reagents and O_2 gas as analyte. *Geochim. Cosmochim. Acta* **61,** 4229–4234.

Santrock J., Studley S. A., and Hayes J. M. (1985) Isotopic analyses based on the mass spectrum of carbon dioxide. *Anal. Chem.* **57,** 1444–1448.

Valley J. W., Kitchen N., Kohn M. J., Niendorf C. R., and Spicuzza M. (1995) UWG-2, a garnet standard for oxygen isotope ratios: strategies for high precision and accuracy with laser heating. *Geochim. Cosmochim. Acta* **59,** 5223–5231.

Van Hook W. A. (1967) Isotope effects on vaporization from the adsorbed state. The methane system. *J. Phys. Chem.* **71,** 3270–3275.

Weichert U. and Hoefs J. (1995) An excimer laser-based micro analytical preparation technique for in-situ oxygen isotope analysis of silicate and oxide minerals. *Geochim. Cosmochim. Acta* **59,** 4093–4101.

Young E. D., Coutts D. W., and D. Kapitan (1998) UV laser ablation and *irm*-GCMS microanalysis of $^{18}O/^{16}O$ and $^{17}O/^{16}O$ with application to a calcium-aluminium-rich inclusion from the Allende meteorite. *Geochim. Cosmochim. Acta* **62,** 3161–3168 (this issue).